


Article

Co-Crystal with Unusual High Z' and Z'' Values Derived from Hexamethylenetetramine and 4-fluorophenol (1/1)

Augusto Rivera ^{1,*}, John Sadat-Bernal ¹, Jaime Ríos-Motta ¹ and Michael Bolte ² 

¹ Universidad Nacional de Colombia, Sede Bogotá, Facultad de Ciencias, Departamento de Química, Síntesis de Heterociclos, Carrera 30 No. 45-03, Bogotá 111321, Colombia; jsbernalg@unal.edu.co (J. S-B.); jariosmo@unal.edu.co (J.R.-M.)

² Institut für Anorganische Chemie, J. W. Goethe-Universität Frankfurt, Max-von Laue-Str., 7, 60438 Frankfurt/Main, Germany; bolte@chemie.uni-frankfurt.de

* Correspondence: ariverau@unal.edu.co; Tel.: +57-1-316-5000

Received: 24 August 2019; Accepted: 9 October 2019; Published: 10 October 2019



Abstract: The title co-crystal, 1,3,5,7-tetraazatricyclo[3.3.1.1^{3,7}]decane (HMTA, 1)–4-fluorophenol (4-FP) (1/1), C₆H₁₂N₄·C₆H₅FO, shows an unusual asymmetric unit that comprises eight independent molecules ($Z'' = 8$), four for each component, with four formula units per asymmetric unit ($Z' = 4$). In the molecular packing, each HMTA molecule bridges one 4-FP molecule via an O–H···N hydrogen bond to form a two-molecule aggregate. Differences can be observed between the bond lengths and angles of the independent HMTA and 4-FP molecules and those of the molecules in the aggregate. The C–N bonds exhibit different bond lengths in the tetrahedral cage-like structure of the HMTA molecules, but the largest differences between the molecular aggregates are in the bond lengths in the 4-fluorophenol ring. In the crystal, the HMTA and 4-FP molecules form two hydrogen-bonded (O–H···N, C–H···F and C–H···O) dimers of HMTA and 4-FP molecules, A···D and B···C inversion dimers, which generate enlarged R₈⁸(34) ring motifs in both supramolecular structures. In both structures, the crystal packing also features additional C–H···F and C–H···O interactions. The A···D and B···C dimers are linked by additional C–H···F and C–H···O hydrogen bonds, forming columns along the *a* and *b* axes, respectively. The importance of the C–H···F interaction to the structure and crystal packing has been demonstrated.

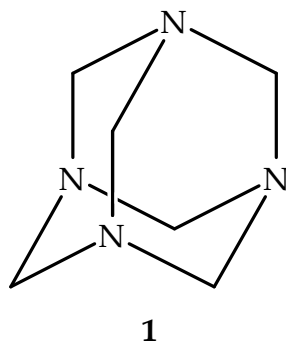
Keywords: crystal structure; urotropine; hydrogen bonding; halogen bonding; C–H···F; mechanochemistry

1. Introduction

Complexes of phenols with various nitrogen bases are model systems often used to study the nature of the hydrogen bond [1]. The hydrogen bonding between the hydroxyl group of acidic species and nitrogen atom of heterocycles has been proven to be a useful and powerful organizing force for the formation of supramolecules [2]. This is a continuation of our previous studies on complexes of phenols with hexamethylenetetramine (**1**, HMTA, Scheme 1), a highly symmetrical molecular scaffold that is attractive due to the presence of four equivalent hydrogen-bond-accepting nitrogen atoms. The hydrogen bonding interactions of hexamethylenetetramine with different types of phenols are interesting, and very few of them have been studied in detail [3]. On the other hand, only seven entries in the Cambridge Structural Database (CSD) include 4-fluorophenol [4]. In this paper, we report the discovery of a new -HMTA:4-fluorophenol co-crystal by mechanochemical grinding. The title structure is the first example of a co-crystal of hexamethylenetetramine with 4-fluorophenol.

Of the various interactions involving halogen atoms, those involving fluorine, the C–H...F hydrogen bonds and F...F interactions, are especially interesting due to the C–H...F structure, which is weak, soft, and flexible, tends to participate in many interactions, and hence, this structural feature reflects in the formation of altered packing motifs due to its substantial effect on the conformation of the molecules [5]. Although still speculative, the recent literature has highlighted the significant role of these weak interactions in crystal packing [6], and a recent investigation established that weak C–H...F–C intermolecular H-bonds were responsible for supramolecular recognition [7]. Of further significance was the fact that these were highly directional interactions that contributed towards the stability of the crystal packing. Single-crystal X-ray analysis of the title compound indicated that the asymmetric unit of the co-crystal, which crystallizes in the triclinic space group P-1, consists of four molecular aggregates, A, B, C, and D ($Z' = 4$) (Figure 1) and eight independent molecules ($Z'' = 8$). The number of molecules (or formula units) in the unit cell is referred to as Z , and the number of symmetry-independent molecules in a crystal structure is referred to as Z' . Formally, Z' is defined as the number of formula units in the crystallographic unit cell divided by the number of independent general positions. Over the past few years, there has been growing interest in crystal structures that contain multiple molecules in the asymmetric unit ($Z' > 1$) [8]. Crystal structures with $Z' > 1$ represent a possible solution to the problem of packing molecules in three dimensions. This phenomenon was comprehensively reviewed in 2015 by Steed and Steed [9], and readers are referred to the Steeds' review for more details. The factors that influence the formation of $Z' > 1$ crystals are unique molecular shapes, small and rigid molecules, enantiopure compounds, strongly directional intermolecular interactions, crystallization factors, solution-phase aggregation, supersaturation and temperature [10]. Additionally, van Eijck et al. referred to Z'' as the total number of chemical entities (independent molecules or ions) in the asymmetric unit [11].

Notably, the structural chemistry aspects of fluorinated organic molecules have been a popular topic in contemporary research because fluorinated organic molecules are broadly applicable in the synthesis of drugs, pharmaceutical products (importantly, fluorine atoms can enhance the pharmacological properties of drugs), and agrochemicals [12].



Scheme 1. Structure of 1,3,5,7-tetraazatricyclo[3.3.1.1^{3,7}]decane (HMTA, 1).

2. Materials and Methods

All reagents were obtained from commercial sources and used without further purification. The melting points were determined with an electrothermal apparatus (Cole-Parmer Lab Apparatus, Stone, Staffordshire, England) using open capillary tubes and are uncorrected. Crystals suitable for X-ray diffraction were obtained from MeOH (Merck KGaA, Darmstadt, Germany) upon the slow evaporation of the solvent at room temperature.

2.1. Preparation of HMTA-4FP Co-Crystals

1,3,5,7-Tetraazatricyclo[3.3.1.1^{3,7}]decane (HMTA, 1) (0.140 g, 1 mmol) (Merck KGaA, Darmstadt, Germany) and 4-fluorophenol (0.112 g, 1 mmol) (Sigma-Aldrich, San Luis, USA) in a 1:1 stoichiometric

ratio were mixed neat and ground manually using an agate mortar and pestle for approximately 15 min. At regular intervals, samples were taken and analysed (TLC). After grinding, crystallization was carried out in 10 mL glass vials in a mixture of chloroform (Merck KGaA, Darmstadt, Germany) and methanol (Merck KGaA, Darmstadt, Germany). Single crystals suitable for X-ray diffraction were obtained in ca. 3 days upon slow evaporation under ambient conditions. Yield: 73%; m. p. = 396 K.

2.2. X-ray Analysis

The X-ray diffraction data were collected on a STOE IPDS II two-circle-diffractometer (STOE & Cie GmbH, Darmstadt, Germany) equipped with MoK α radiation ($\lambda = 0.71073 \text{ \AA}$) at 173(2) K in ω scan mode. Unit cell refinement was conducted using X-Area software (Stoe & Cie, Darmstadt, Germany) [13]. The structure was solved by direct methods using SHELX-2016/6 [14]. For structural refinement [14], the nonhydrogen atoms were treated anisotropically, the hydrogen atoms bound to O were refined isotropically, and the remaining H atoms were treated as riding. Crystallographic data were deposited at the Cambridge Crystallographic Data Centre (CCDC). Copies of the data can be obtained free of charge upon application to the CCDC, 12 Union Road, Cambridge CB2 IEZ, UK. Fax: +44-(0)1223-336033 or e-mail: deposit@ccdc.cam.ac.uk. The CCDC deposition number is 1949826. Selected crystallographic data and details concerning data collection and structure refinement are given in Table 1.

Table 1. Crystal data and structure refinement for HMTA-4-FP 1:1 co-crystal.

CCDC No.	1949826
Empirical formula	C ₆ H ₁₂ N ₄ ·C ₆ H ₅ FO
Formula weight	252.29
Temperature	173(2) K
Crystal system	triclinic
Space group	<i>P</i> 1
Unit cell dimensions	$a = 10.1873(10) \text{ \AA}, \alpha = 96.068(7)^\circ$
	$b = 10.2048(9) \text{ \AA}, \beta = 96.058(8)^\circ$
	$c = 23.554(2) \text{ \AA}, \gamma = 90.179(8)^\circ$
Volume	2421.1(4)Å ³
Z	8
Calculated density	1.384 g/cm ³
Absorption coefficient	0.10 mm ⁻¹
F(000)	1072
Crystal size mm ³	0.28 × 0.27 × 0.27
$\theta_{\min}/\theta_{\max}/^\circ$	1.8/25.0
Limiting indices	$-12 \leq h \leq 12, -12 \leq k \leq 12, -28 \leq l \leq 28$
Reflections collected	8402
Independent reflections	8402
Refinement method	Full-matrix least-squares on F^2
Data/restraints/parameters	8402/0/657
Goodness of fit on F^2	1.941
$R1/wR2[I > 2\sigma(I)]$	0.1076/0.2724
$R1/wR2(\text{all data})$	0.1442/0.2931
Largest diff. peak and hole/e.Å ⁻¹	0.580 / -0.482

3. Results and Discussion

Single Crystal X-Ray Diffraction

X-ray crystallography reveals the title co-crystal to comprise 1,3,5,7-tetraazatricyclo[3.3.1.1^{3,7}]decane (HMTA, 1) and 4-fluorophenol (4-FP) in the ratio 1:1, but with four crystallographically nonequivalent HMTA molecules and four crystallographically nonequivalent 4-FP molecules in the asymmetric unit (Figure 1). Thus, the co-crystal crystallizes in the triclinic space group *P*-1 with four molecular aggregates in the asymmetric unit ($Z' = 4$), viz. aggregates A, B, C and D; and eight independent molecules ($Z'' = 8$). Contrary to other structures with $Z' > 1$, no appreciable differences between the conformations of the four symmetrically independent co-crystals can be observed.

The molecular structure of the four crystallographically independent two-molecule aggregates forming the asymmetric unit of the crystal structure of the title compound is shown in Figure 1. Molecular aggregates B–D all have a 1:1 ratio, and all have N...H–O–hydrogen bonds between the two species but differ in their structural parameters and crystal packing, as described below. Although the 4-FP:HMTA adduct is a 1:1 two-molecule aggregate of a phenol and HMTA, similar to the co-crystal of 2,4,6-trinitrophenol and 4-hydroxy-3-methoxybenzaldehyde with a hydrogen-bonded co-crystal involving monodonor molecules and using one N atom in the molecule of HMTA [15], the title compound is the first case that crystallizes with more of one molecule in the asymmetric unit, which is an intriguing structural parameter indicated by the X-ray diffraction studies.

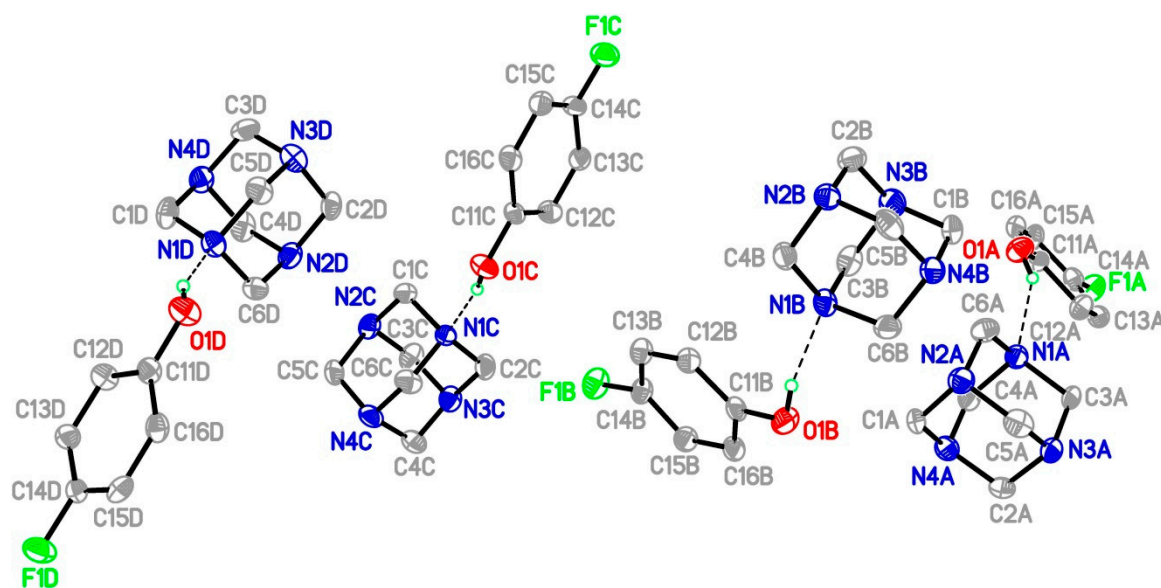
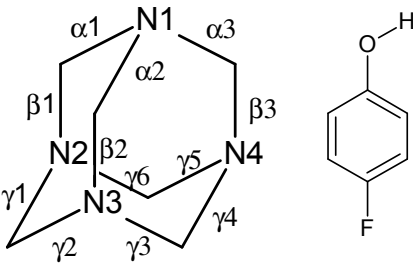


Figure 1. Perspective view of the asymmetric unit of the title compound. H atoms not involved in hydrogen bonds are omitted for clarity. The displacement ellipsoids are drawn at the 30% probability level.

To a first approximation, the structure of A resembles those of B–D. However, although the HMTA molecules are structurally rigid due to the absence of conformational flexibility, we observed that the molecules are crystallographically nonequivalent due to differences in the C–N bond lengths. This is evidenced by the differences in lengths of the C–N bonds around the nitrogen atoms involved in the hydrogen bonds with the 4-FP molecules, hereafter referred to as α bonds, which range from 1.476(9) to 1.493(10) Å, 1.462(10) to 1.500(10) Å, 1.442(10) to 1.504(10) Å and 1.468(10) to 1.504(10) Å for the A–D HMTA molecules. The lengths of these bonds (except for the α_3 bond in C, Table 2), are relatively longer on average than those of HMTA itself (1.462(5) Å) [16]. In addition, adjacent C–N bonds (referred to as β) are generally shorter relative to HMTA, ranging from 1.445(10) to 1.456(10) Å, 1.452(10) to 1.469(10) Å, 1.443(11) to 1.494(10) Å and 1.431(10) to 1.481(10) Å for the A–D HMTA molecules,

which is consistent with an anomeric effect [17]. However, comparing the bond lengths observed for A–D to those of previous studies reported in the literature for the O–H⋯N hydrogen-bonded aggregate of HMTA with hydroxybenzoic acid [17], we found that not all the β bonds are shorter than the corresponding α bonds and the bond in HMTA, for example, $\alpha 2$ and $\beta 2$ in B, $\beta 3$ and $\beta 3$ in C and $\beta 1$ and $\beta 2$ in D (Table 2). However, the most significant differences in the N–C bond lengths within the four HMTA molecules appear at the other six N–C bonds involving the carbon atoms attached to two different nitrogen atoms (excluding N1), named γ bonds. The $\gamma 6$ in D and $\gamma 3$ and $\gamma 5$ bonds in C are significantly shorter than the N–C bonds of the uncomplexed HMTA or those of the 1:1 hydroxybenzoic acid adduct (1.460(2) to 1.480(6)) [17]. On the other hand, the $\gamma 4$ and $\gamma 5$ bonds in D are longer than those in the 1:1 hydroxybenzoic acid adduct. The average values of all N–C bond lengths in the HMTA moiety are 1.469, 1.469, 1.466 and 1.473 Å for A, B, C and D, respectively. Despite these variations, the intra-ring bond angles in the HMTA rings of the four aggregates are not very different, with average values of the C–N–C bond angles of 108.0°, 107.7°, 107.8° and 108.0° for the A, B, C and D units of HMTA, respectively, and N–C–N bond angles of 112.3°, 112.7°, 112.6° and 112.4°, respectively. In the same way, and similar to the 1:1 co-crystal of HMTA with 4-hydroxy-3-methoxybenzaldehyde [18], the puckering parameters [19] for the four six-membered N–C–N–C–N–C rings of each HMTA molecule span an experimentally equivalent range, with a mean deviation of all atoms from their mean-ring planes of 0.236 for A and D and 0.235 for B and C. The abovementioned ring puckering data indicate that the bond-length variations do not alter the intra-ring angles and the tetrahedral cage-like structure in the four HMTA molecules.

Table 2. Selected bond lengths and angles for HMTA:4-FP 1:1 adduct [distances in Å and bond angles and torsion angles in degrees].



Parameter	A	B	C	D	HMTA	4-FP
$\alpha 1$	1.486(10)	1.500(10)	1.498(9)	1.472(10)		
$\alpha 2$	1.476(9)	1.462(10)	1.504(10)	1.504(10)		
$\alpha 3$	1.493(10)	1.482(9)	1.442(10)	1.468(10)		
$\beta 1$	1.445(10)	1.460(10)	1.466(11)	1.481(10)		
$\beta 2$	1.456(10)	1.469(11)	1.443(11)	1.431(10)		
$\beta 3$	1.446(10)	1.452(10)	1.494(10)	1.472(11)		
$\gamma 1$	1.482(10)	1.470(10)	1.484(10)	1.468(10)	1.462(5) ^a	
$\gamma 2$	1.469(11)	1.469(10)	1.466(10)	1.467(10)		
$\gamma 3$	1.475(11)	1.467(10)	1.427(11)	1.478(10)		
$\gamma 4$	1.469(10)	1.467(10)	1.460(11)	1.489(11)		
$\gamma 5$	1.463(11)	1.473(10)	1.443(10)	1.493(11)		
$\gamma 6$	1.472(11)	1.458(10)	1.465(10)	1.448(10)		
F1—C14	1.395(8)	1.366(8)	1.360(8)	1.378(8)		1.361 ^b ; 1.3406 ^c
O1—C11	1.372(9)	1.372(9)	1.359(9)	1.358(9)		1.380 ^b ; 1.3651 ^c
C13—C14	1.383(10)	1.378(10)	1.385(10)	1.361(10)		1.365, 1.368 ^b ; 1.3864, 1.3890 ^c
C14—C15	1.350(10)	1.385(10)	1.366(10)	1.379(10)		1.365, 1.368 ^b ; 1.3864, 1.3890 ^c
C12—C13	1.417(10)	1.387(10)	1.393(10)	1.398(10)		1.379 ^b ; 1.3958 ^c
C15—C16	1.400(11)	1.401(11)	1.394(11)	1.385(11)		1.379 ^b ; 1.3925 ^c

References: a: [16]; b: [20] and c: [21].

However, the bond lengths in the four 4-fluorophenol rings are different. For example, the F–C bond lengths for the A and D 4-fluorophenol molecules, 1.395(8) and 1.378(8) Å, respectively, are relatively longer than the equivalent bonds in B and C and those of 4-fluorophenol (1.361 Å) [20]. This is also seen in the greater disparity in the associated C13–C14 and C14–C15 bond lengths (Table 2). We also observed that these bonds are relatively longer than those of 4-FP (1.365 and 1.368 Å) [20,21]. Additionally, an inspection of the other C–C bond lengths, as seen in Table 2 for 4-FP molecules, shows that there is a slight asymmetry in the electronic distribution around the aromatic ring of the 4-FP molecules. For example, C12–C13 and C15–C16 are slightly elongated in comparison to 4-FP [20,21]. Furthermore, the marked discrepancy between C13–C14 and C14–C15 with respect to the C12–C13 and C15–C16 distances, with the later being significantly longer in all cases, reflects a decrease in the contribution of the quinoid-type structure in the 4-FP rings [21]. This is consistent with an increase in the σ -electron-withdrawing (inductive) effect of the fluorine substituent on the four independent molecules of 4-FP [21].

Although 4-fluorophenol is supposed to form intermolecular C–H...F hydrogen bonds, it is well known that the formation of these intermolecular hydrogen bonds with fluorine as an acceptor is possible in environments shielded from water and with no competing hydrogen-bond acceptors [22,23]. However, similar to C–H...O hydrogen bonds [24,25], the stabilization energy of the C–H...F interactions (< 5 kcal/mol) [26] in the crystal lattice can compete with conformational forces and are responsible for the other structural changes in small molecules. In these cases, the close C–H...F contacts could play an important role in crystal packing [12,22,27–30].

As indicated in PLATON [31], the crystal structure features four O–H...N hydrogen bonds (Table 3). These bonds occur such that each molecule of HMTA links one 4-FP molecule to form four two-molecule aggregates, as illustrated in Figure 1. These aggregates are connected into a three-dimensional architecture by a large number of C–H...X interactions (X = F, O and N).

Table 3. Hydrogen bonds in the co-crystal [Å and °].

D-H...A	d(D-H)	d(H...A)	d(D...A)	<(DHA)
O(1A)-H(1A)...N(1A)	0.84	1.98	2.741 (8)	151
O(1B)-H(1B)...N(1B)	0.84	1.92	2.740 (8)	166
O(1C)-H(1C)...N(1C)	0.84	1.93	2.756 (8)	169
O(1D)-H(1D)...N(1D)	0.84	1.94	2.739 (8)	158
C(5B)-H(5B1)...O(1C)#1	0.99	2.54	3.505(10)	166
C(5A)-H(5A1)...O(1D)#1	0.99	2.56	3.521(10)	164
C(4C)-H(4C1)...O(1B)#2	0.99	2.59	3.567(11)	168
C(3D)-H(3D2)...O(1A)#3	0.99	2.56	3.529(10)	167
C(1D)-H(1D1)...F(1A) #4	0.99	2.41	3.200(10)	136
C(3A)-H(3A2)...F(1D) #5	0.99	2.40	3.199(9)	137
C(12D)-H(12D)...F(1A) #6	0.95	2.55	3.190(8)	125
C(12C)-H(2C2)...F(1B)	0.99	2.45	3.219(9)	134
C(4B)-H(4B2)...F(1C) #7	0.99	2.45	3.224(9)	135
C(4A)-H(4A1)...N(2C) #6	0.99	2.62	3.589(10)	165

Symmetry codes: #1 $-x + 1, -y, -z + 1$; #2 $-x, -y, -z + 1$; #3 $-x + 1, -y + 1, -z + 1$; #4 $x + 1, y, z + 1$; #5 $x, y, z - 1$; #6 $-x, -y + 1, -z + 1$; #7 $x, y - 1, z$.

In the crystal, the two-molecule aggregates A and D are linked via a pair of C–H...F and C–H...O hydrogen bonds forming an inversion dimers with enlarged $R_8^8(34)$ ring motifs (named A–D). Similar interactions between B and C aggregates forming a second $R_8^8(34)$ ring motifs (named B–C). For example, for A–D supramolecular synthons, pairs of C(1D)–H(1D1)...F(1A) and C(5A)–H(5A1)...O(1D) interactions operate in conjunction with O(1A)–H(1A)...N(1A) and O(1D)–H(1D)...N(1D) hydrogen bonds to close a thirty-four-membered synthon (Figure 2). These inversion dimers are connected into chains propagating along the *a* axis by two additional C–H...F interactions, (C(3A)–H(3A2)...F(1D) and C(12D)–H(12D)...F(1A)) and one C(3D)–H(3D2)...O(1A)

hydrogen bond (Figure 3). The chains are reinforced by aromatic $\pi\cdots\pi$ stacking [$Cg29\cdots Cg29 = 4.029(4)$ Å and $Cg32\cdots Cg32 = 4.037(4)$ Å; $Cg29$ and $Cg32$ are the centroids of the C11A–C16A and C11D–C16D rings, respectively] (Figure 4).

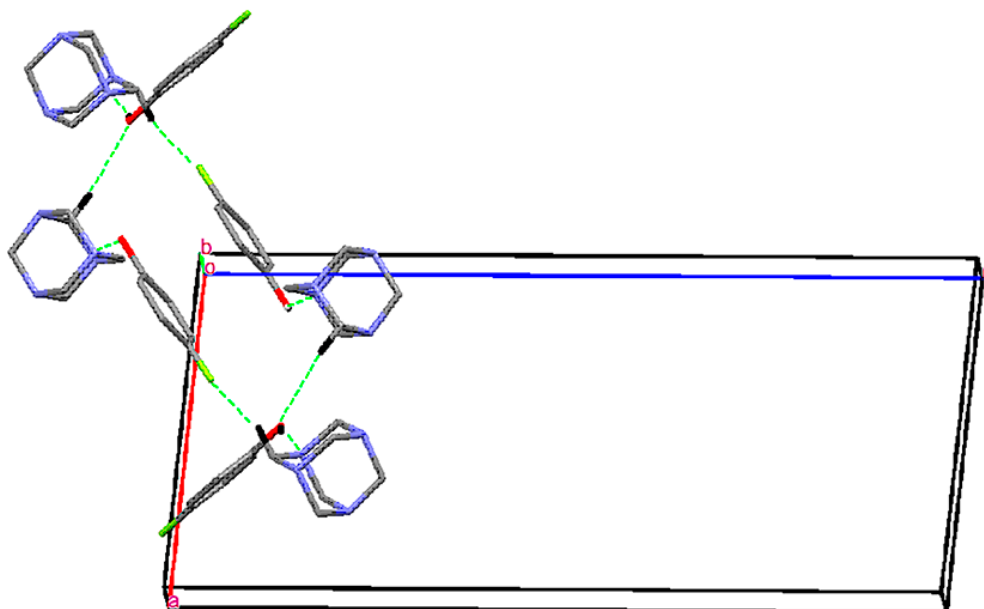


Figure 2. The view of the enlarged $R_8^8(34)$ ring motifs along the b axis, showing the participation of $O-H\cdots N$, $C-H\cdots F$ and $C-H\cdots O$ (Table 3) in the formation of the A–D ring inversion dimer.

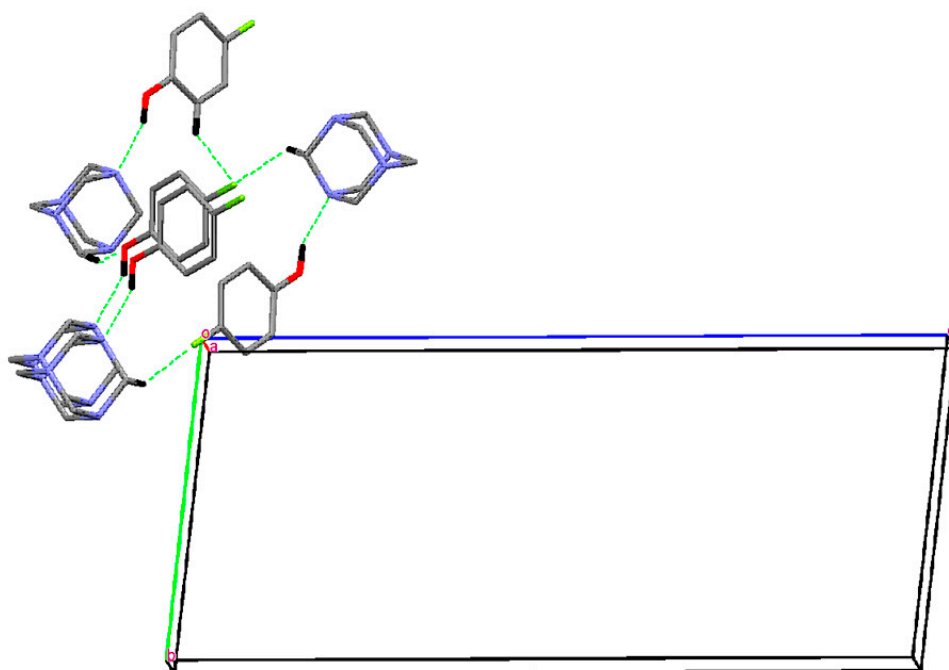


Figure 3. A view along the a axis of the part of the crystal packing of the title compound, showing the formation of columns of the A–D ring inversion dimer. For clarity, only hydrogen atoms involved in hydrogen bond interactions have been included.

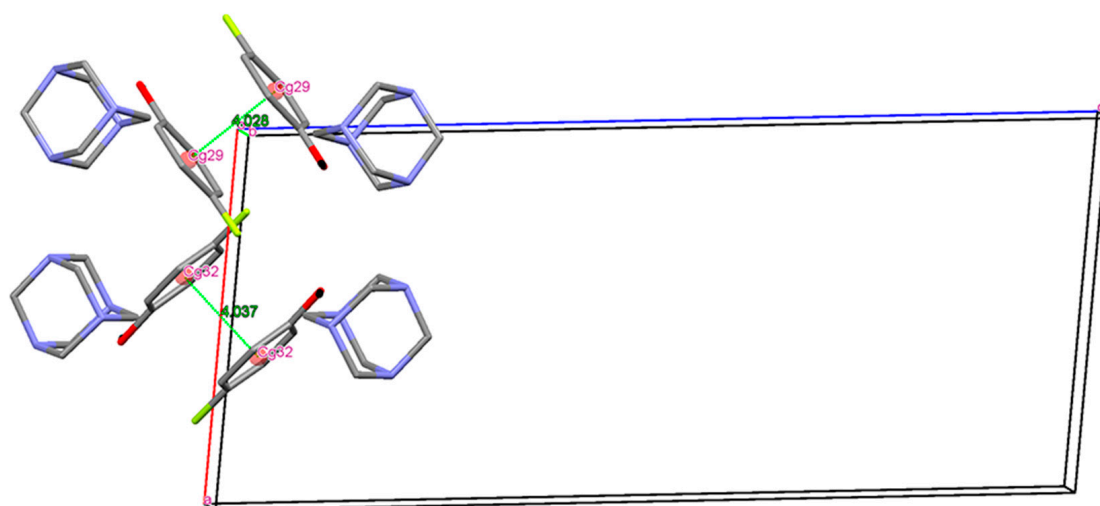


Figure 4. A view along the *b* axis of the part of the crystal packing of title compound showing the $\pi\cdots\pi$ stacking. Distances are given in Å. Hydrogen atoms are omitted for clarity.

Although in principle, symmetry-independent molecules must have different supramolecular networking, the hydrogen-bonding pattern in the B–C inversion dimer is similar to that observed in the A–D inversion dimer, but with different geometric parameters (Table 3). Unlike in the A–D inversion dimer, each fluorine atom has only one contact with a hydrogen atom, while in the A–D dimer, F1 is in contact with two hydrogen atoms (Table 3). There are two C–H \cdots F and two C–H \cdots O hydrogen bonds that are slightly longer than those in the crystal structure of the A–D inversion dimer and form columns in the $R_8^8(34)$ inversion dimer with different orientations along the *b* axis (Figure 5), which is also controlled by weak aromatic $\pi\cdots\pi$ stacking interactions [centroid–centroid separations = 4.025(4) and 4.037(4) Å]. Furthermore, both columns are linked by a weak hydrogen bond (C(4A)–H(4A1) \cdots N(2C), Table 3) that contributes to the crystal packing, forming a three-dimensional structure.

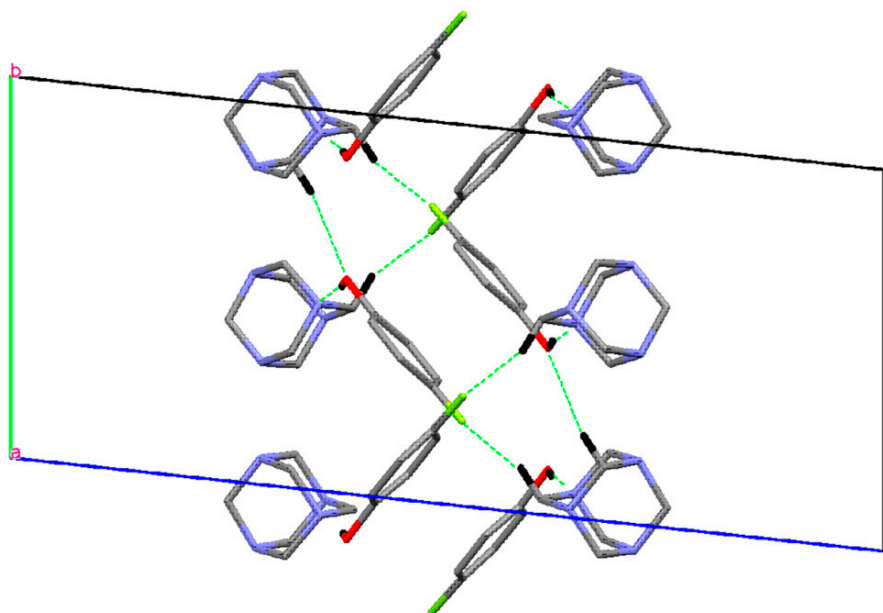


Figure 5. A view along the *a* axis of part of the crystal packing of the title compound showing the formation of columns of the B–C $R_8^8(34)$ inversion dimer. For clarity, only hydrogen atoms involved in hydrogen bond interactions have been included.

The most prominent feature of the molecular packing in the crystal of the title 1:1 adduct is the formation of the four two-molecule aggregates with different structural parameters (F–C, N–C, O–C and C–C bond lengths, Table 2) and different hydrogen bonds with geometric parameters (Table 3). In fact, although the hydrogen-bonding patterns are almost identical, there are differences in the donor–acceptor distances, which range from 3.567(11) to 3.505(10) Å for C–H···O hydrogen bonds and 3.190(8) to 3.224(9) Å for C–H···F hydrogen bonds. Thus, one might expect any C–H···O and C–H···F contacts to be different for the four two-molecule aggregates. However, the C···F distances are only 0.02 and 0.03 Å longer than the sum of the van der Waals radii (F = 1.47 Å, C = 1.70 Å) [32] for the A and D two-molecule aggregate, while the interactions in B and C are 0.05 Å longer. On the other hand, the four C–H···O hydrogen bonds are longer than the sum of the van der Waals radii (O = 1.52 Å, C = 1.70 Å) [32] by 0.31, 0.35, 0.28 and 0.25 Å (Table 3). Based on their lengths, these are presumably significantly weaker than the C–H···F hydrogen bonds.

Compared to the F–C bond length of 1.361 Å in 4-fluorophenol, as stated before, we believe that the intermolecular C–H···F–C hydrogen bonding interaction is the key to the observed structural changes, especially the observation of these elongated F–C bonds, which include the F1A–C14A, F1C–C14C, F1A–C14A, and F1D–C14D bonds. The plot of F–C bond length versus C···F distance is shown in Figure 6. The F–C bond length almost linearly increases with decreasing donor–acceptor distance (C···F distance). The presence of two C–H···F hydrogen bond interactions in F1 made the F–C distance notably longer. Thus, the F1A atom is distinct from the F1(B–D) atoms based on the number of interactions it forms.

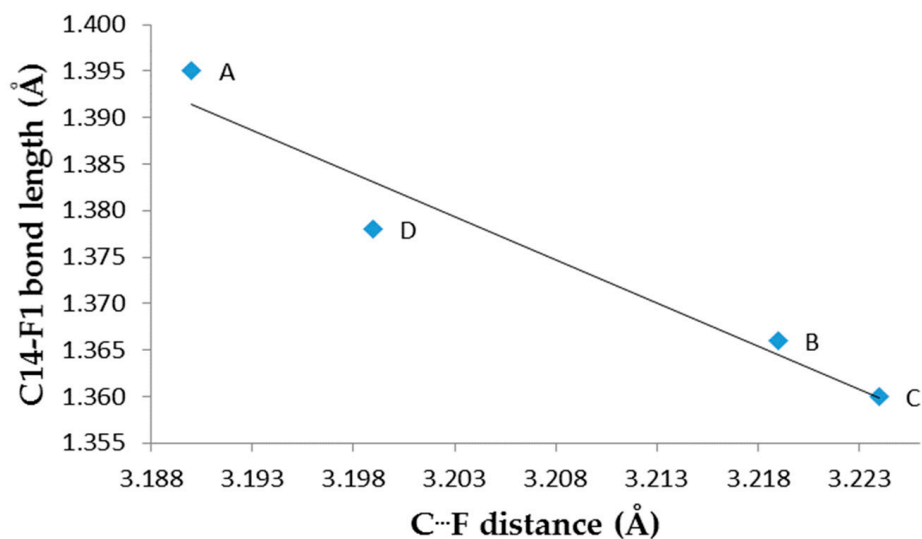


Figure 6. C–F Bond lengths versus donor–acceptor distances for the four two-molecule aggregates.

In conclusion, we have shown that the addition of one fluorine atom at the para position on the phenolic ring has influence in the generation of supramolecular assemblies in HMTA-phenol adducts. The altered packing modes due to the nature of the interactions, such as the different weak intermolecular C–H···F–C hydrogen bonds, influence the crystal structure of this co-crystal. Unlike what is typical for structures with $Z' > 1$, no appreciable differences between the conformations of the four symmetrically independent co-crystals could be observed.

Author Contributions: A.R. conceived and designed the experiments; J.S.B. performed the experiments; M.B. collected X-ray data and solved the X-ray structure; A.R. and J.R.-M. wrote the paper.

Funding: This research was funded by Dirección de Investigaciones, Sede Bogotá (DIB) de la Universidad Nacional de Colombia (Grant No. 35816).

Acknowledgments: We acknowledge the Dirección de Investigaciones, Sede Bogotá (DIB) de la Universidad Nacional de Colombia, for financial support of this work (Grant No. 35816).

Conflicts of Interest: The authors declare no conflict of interest.

References

1. Majerz, I.; Kwiatkowska, E.; Koll, A. The influence of hydrogen bond formation and the proton transfer on the structure of complexes of phenols with N-methylmorpholine. *J. Mol. Struct.* **2007**, *831*, 106–113. [[CrossRef](#)]
2. Jin, S.; Liu, H.; Gao, X.J.; Lin, Z.; Chen, G.; Wang, D. Seven organic salts assembled from hydrogen-bonds of N–H···O, O–H···O, and C–H···O between acidic compounds and bis(benzimidazole). *J. Mol. Struct.* **2014**, *1075*, 124–138. [[CrossRef](#)]
3. Vijayalakshmi, S.; Kalyanaraman, S. Non linear optical analyses of hexamine: Phenol co-crystals based on hydrogen bonding: A comparative study. *Spectrochim. Acta A* **2014**, *120*, 14–18. [[CrossRef](#)] [[PubMed](#)]
4. Groom, C.R.; Bruno, I.J.; Lightfoot, M.P.; Ward, S.C. The Cambridge Structural Database. *Acta Cryst. B* **2016**, *72*, 171–179. [[CrossRef](#)] [[PubMed](#)]
5. Cetina, M.; Benci, K.; Wittine, K.; Mintas, M. Weak C–H··· π and C–H···F interactions form higher-order supramolecular structures in cytosine and uracil (Z)-4'-benzamido-2'-butenyl derivatives. *Cryst. Growth. Des.* **2012**, *12*, 5262–5270. [[CrossRef](#)]
6. Hathwar, V.R.; Chopra, D.; Panini, P.; Guru Row, T.N. Revealing the polarizability of organic fluorine in the trifluoromethyl group: Implications in supramolecular chemistry. *Cryst. Growth. Des.* **2014**, *14*, 5366–5369. [[CrossRef](#)]
7. Chopra, D. Is organic fluorine really “not” polarizable? *Cryst. Growth. Des.* **2012**, *12*, 541–546. [[CrossRef](#)]
8. Chattopadhyay, B.; Hemantha, H.P.; Narendra, N.; Sureshababu, V.V.; Warren, J.E.; Helliwell, M.; Mukherjee, A.K.; Mukherjee, M. Polymorphism in a symmetrical dipeptidyl urea with $Z' > 1$. *Cryst. Growth. Des.* **2010**, *10*, 2239–2246. [[CrossRef](#)]
9. Steed, K.M.; Steed, J.W. Packing problems: High Z' crystal structures and their relationship to co-crystals, inclusion compounds, and polymorphism. *Chem. Rev.* **2015**, *115*, 2895–2933. [[CrossRef](#)] [[PubMed](#)]
10. Bombicz, P. The way from isostructurality to polymorphism. Where are the borders? The role of supramolecular interaction and crystal symmetries. *Cryst. Rev.* **2017**, *23*, 118–151. [[CrossRef](#)]
11. Van Eijck, B.P.; Kroon, J. Structure predictions allowing more than one molecule in the asymmetric unit. *Acta Cryst. B* **2000**, *56*, 535–542. [[CrossRef](#)] [[PubMed](#)]
12. Yadav, H.R.; Choudhury, A.R. Can C–H···F–C hydrogen bonds alter crystal packing features in the presence of N–H···O–C hydrogen bond? *J. Mol. Struct.* **2017**, *1150*, 469–480. [[CrossRef](#)]
13. Stoe & Cie. *X-Area Diffractometer Control Software*; Stoe & Cie: Darmstadt, Germany, 2001.
14. Sheldrick, G.M. Crystal structure refinement with SHELXL. *Acta Cryst. C* **2015**, *71*, 3–8. [[CrossRef](#)] [[PubMed](#)]
15. Lemmerer, A. Seven hexamethylenetetramine (HMTA) complexes with mono- and dicarboxylic acids: Analysis of packing modes of HMTA complexes in the literature. *Acta Cryst. B* **2011**, *67*, 177–192. [[CrossRef](#)] [[PubMed](#)]
16. Terpstra, M.; Craven, B.M.; Stewart, R.F. Hexamethylenetetramine at 298 K: New refinements. *Acta Cryst. A* **1993**, *49*, 685–692.
17. Chandrasekhar, S.; Mukherjee, S. Salts of hexamethylenetetramine with organic acids: Enhanced anomeric interactions with a lowering of molecular symmetry revealed by crystal structures. *J. Mol. Struct.* **2015**, *1082*, 188–194. [[CrossRef](#)]
18. Usman, A.; Chantrapromma, S.; Fun, H.K.; Poh, B.L.; Karalai, C. A 1:1 adduct of hexamethylenetetramine and 4-hydroxy-3-methoxybenzaldehyde. *Acta Cryst. C* **2002**, *58*, o48–50. [[CrossRef](#)]
19. Cremer, D.; Pople, J.A. General definition of ring puckering coordinates. *J. Am. Chem. Soc.* **1975**, *97*, 1354–1355. [[CrossRef](#)]
20. Oswald, D.H.; Allan, D.R.; Day, G.M.; Samuel Motherwell, W.D.; Parsons, S. Realizing predicted crystal structures at extreme conditions: The low-temperature and high-pressure crystal structures of 2-chlorophenol and 4-fluorophenol. *Cryst. Growth. Des.* **2005**, *53*, 1055–1071. [[CrossRef](#)]
21. Zierkiewicz, W.; Michalska, D.; Czarnik-Matusiewicz, B.; Rospenk, M. Molecular structure and infrared spectra of 4-fluorophenol: A combined theoretical and spectroscopic study. *J. Phys. Chem. A* **2003**, *107*, 4547–4554. [[CrossRef](#)]

22. Dalvit, C.; Invernizzi, C.; Vulpetti, A. Fluorine as a hydrogen-bond acceptor: Experimental evidence and computational calculations. *Chem. Eur. J.* **2014**, *20*, 11058–11068. [[CrossRef](#)] [[PubMed](#)]
23. Gamekkanda, J.C.; Sinha, A.S.; Desper, J.; Daković, M.; Aakeröy, C.B. Competition between hydrogen bonds and halogen bonds: A structural study. *New J. Chem.* **2018**, *42*, 10539–10547. [[CrossRef](#)]
24. Desiraju, G.R. The C–H···O Hydrogen bond in crystals: What is it? *Acc. Chem. Res.* **1991**, *24*, 290–296. [[CrossRef](#)]
25. Steiner, T. C–H···O hydrogen bonding in crystals. *Cryst. Rev.* **2003**, *9*, 177–228. [[CrossRef](#)]
26. Cavallo, G.; Metrangolo, P.; Milani, R.; Pilati, T.; Priimagi, A.; Resnati, G.; Terraneo, G. The halogen bond. *Chem. Rev.* **2016**, *116*, 2478–2601. [[CrossRef](#)] [[PubMed](#)]
27. Chakraborty, S.; Desiraju, G.R. C–H···F Hydrogen bonds in solid solutions of benzoic acid and 4-fluorobenzoic acid. *Cryst. Growth. Des.* **2018**, *18*, 3607–3615. [[CrossRef](#)]
28. Hu, Y.; Hu, H.; Li, Y.; Chen, R.; Yang, Y.; Wang, L. Supramolecular assemblies of tetrafluoroterephthalic acid and N-heterocycles via various strong hydrogen bonds and weak C–H···F interactions: Synthons cooperation, robust motifs and structural diversity. *J. Mol. Struct.* **2016**, *1122*, 256–267. [[CrossRef](#)]
29. Horiguchi, M.; Okuhara, S.; Shimano, E.; Fujimoto, D.; Takahashi, H.; Tsue, H.; Tamura, R. Control of the mode of polymorphic transition inducing preferential enrichment by modifying the molecular structure or adding seed crystals: Significant influence of CH/F hydrogen bonds. *Cryst. Growth. Des.* **2008**, *8*, 540–548. [[CrossRef](#)]
30. Rivera, A.; Rojas, J.J.; Ríos-Motta, J.; Bolte, M. Crystal structure and C–H···F hydrogen bonding in the fluorinated bis-benzoxazine: 3,3'-(ethane-1,2-diyl)bis(6-fluoro-3,4-dihydro-2H-1,3-benzoxazine). *Acta Cryst. E* **2016**, *72*, 1509–1511. [[CrossRef](#)]
31. Spek, A.L. Structure validation in chemical crystallography. *Acta Cryst. D* **2009**, *65*, 148–155. [[CrossRef](#)]
32. Bondi, A. Van der Waals volumes and radii. *J. Phys. Chem.* **1964**, *68*, 441–451. [[CrossRef](#)]



© 2019 by the authors. Licensee MDPI, Basel, Switzerland. This article is an open access article distributed under the terms and conditions of the Creative Commons Attribution (CC BY) license (<http://creativecommons.org/licenses/by/4.0/>).